ELSEVIER

Journal of Nuclear Materials 301 (2002) 118–121

journal of nuclear materials

www.elsevier.com/locate/jnucmat

Hardness and microstructural studies of electron beam welded joints of Zircaloy-4 and stainless steel

M. Ahmad [a,*], J.I. Akhter [a], M.A. Shaikh [a], M. Akhtar [a], M. Iqbal [a], M.A. Chaudhry [b]

[a] *Nuclear Physics Division, Pakistan Institute of Nuclear Science and Technology, P.O. Nilore, Islamabad, Pakistan*

[b] *Applied Physics Division, Pakistan Institute of Nuclear Science and Technology, P.O. Nilore, Islamabad, Pakistan*

Received 20 June 2001; accepted 30 November 2001

Abstract

Electron beam welded joints between Zircaloy-4 and stainless steel 304L are investigated due to their importance in the nuclear industry. The molten and heat affected zones (HAZs) are found to be free of defects. Diffusion of Fe, Cr and Ni is observed in Zircaloy-4 near the molten zone and of Zr and Sn in the stainless steel. A rod-shaped intermetallic compound $Zr(Cr,Fe)_2$ and eutectic phases $ZrCr_2$–liquid (Zr,Fe) and Zr_2Fe–Zr_2Ni are present in the molten zone. The hardness of the molten zone, containing $Zr(Cr,Fe)_2$, is much higher than the rest of the molten zone and the HAZs.

1. Introduction

Zircaloy-4 is used as a cladding material for fuel elements in thermal reactors [1]. Stainless steel is used as structural material in the nuclear industry due to its cost effectiveness compared to Zircaloy [2]. There are many joints/contacts between structural material and cladding material in some reactors. For example, in pressurised heavy water reactors such joints are between pressure tube/end fitting, calandria tube/tube sheet of calandria vessel and temperature monitor assemblies [3]. The interaction between Zircaloy and stainless steel has been a subject of many studies in the past due to its importance in the nuclear industry [4–7]. The joint between these two alloys has been tried in many ways because the welding of dissimilar alloys is always problematic. Mukherjee and Panakkal [8] studied the interaction between SS-302 springs and Zircaloy-4 produced by tungsten inert gas welding and showed that brittle intermetallics and cracks were formed in the weld region. Zhou Hairong and Zhou Bangxin [9] investigated the microstructure of explosive welded joints between Zircaloy-4 and stainless steel and observed a crystalline phase $Zr(Fe,Cr)_2$ with hexagonal structure and concluded that the welded joints could be pulled, bent and cold rolled without crack formation on the bonding layer because the molten regions were small and distributed as isolated islands.

Electron beam welding, on the other hand, has many advantages over the other welding techniques. This is a fusion joining process that produces coalescence of the materials with heat from a high energy electron beam focused on the weld joints. This process is carried out in vacuum and the beam can be focused on a small area. Thus the materials can be joined together in a short time and it reduces the long-range flow of heat and defects like voids, cracks and oxidation may be avoided. There is little literature available on the interactions of stainless steel and Zircaloy-4 produced by electron beam welding. In the present study we report different phases and microstructure of the fusion and heat affected zones from samples of Zircaloy-4 and stainless steel 304L joined together by electron beam.

* Corresponding author.

E-mail addresses: jiakhter@yahoo.com, akhterji@hotmail.com (J.I. Akhter).

0022-3115/02/$ - see front matter
PII: S0022-3115(01)00757-7

Table 1
Nominal composition of alloys

Alloys	Elements in wt%							
	Sn	Cr	Ni	Si	C	Mn	Fe	Zr
Zircaloy-4	1.52	0.1	<0.005	–	0.002	–	0.2	Bal.
Stainless steel 304L	–	19.0	10.0	1.0	0.03	2.0	Bal.	–

2. Experimental

The nominal composition of stainless steel 304L and Zircaloy-4 are given in Table 1. Stainless steel was obtained in the form of a sheet having a thickness of 2 mm. The sheet was rolled to 1 mm at 900 °C. Three samples of dimensions of $2 \times 1 \times 0.1$ cm^3 were cut from the sheet of rolled stainless steel. Samples of the same dimension were also cut from the sheet of Zircaloy-4. Surfaces of the samples were polished on a lapping machine using diamond paste down to 0.25 μm. Joining sides of both metals were also polished up to the same level. The samples were placed together in a special die to hold them in such a way that they could not separate from each other during the course of welding. A locally designed and manufactured machine was used to join the materials. Electron beam welding was carried out in high vacuum of 1.3×10^{-8} bar with a voltage of 10 kV, current of 40 mA, and time varying from 2.5 to 4 min. After welding the samples were again polished and etched chemically in a solution of H_2O_2:HNO_3:HF with a volume ratio of 50:47:3 having strength of 35%, 63% and 40%, respectively. The microstructure was investigated by scanning electron microscopy (SEM) and the phases were characterized by electron probe microanalysis (EPMA). Microhardness (Vickers) values of the different regions were determined using a load of 1.96 N at room temperature.

3. Results and discussion

SEM examination of the welded samples at low magnification reveals the occurrence of two distinct regions, i.e. a molten zone and a heat affected zone (HAZ) as shown in Fig. 1. The HAZ is expected on both sides of the molten zone. However, it is distinctly observed on the side of stainless steel only. The HAZ on the side of stainless steel is rich in Cr and depleted in Ni compared to the original composition of stainless steel. The micrograph and line scan shown in Fig. 2(a) and (b), give variation of Zr, Ni, Fe, and Cr in this area. No HAZ with distinct contrast was observed on the side of Zircaloy-4 because of little diffusion of Ni, Fe and Cr towards this material beyond the molten zone.

Steel and zirconium form a multinary eutectic system during cooling from liquid to solid. During cooling even

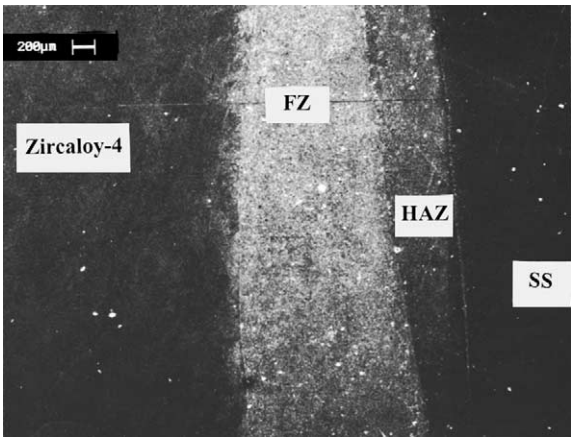

Fig. 1. SEM micrograph showing the two distinct regions.

from high temperature by crossing the liquid line, precipitations of Laves phases ZrM_2 (M being Fe, Cr, Ni) have been reported [10]. The molten zone consists of two regions. The region near the HAZ, on the side of stainless steel, shows rod shape particles with black contrast. Their average composition is given in Table 2 which suggests that these are intermetallic compounds of the $Zr(Cr,Fe)_2$ type. A variation in the concentration of the Fe, Cr and Zr in these particles is observed. The matrix around these particles is rich in Zr, Fe and Ni and the average composition of this eutectic is also given in Table 2. Small size particles rich in Zr, with low amounts of Fe, Sn and Ni are also observed throughout the molten zone. The region on the side of the Zircaloy-4 has large areas with a dendritic structure and is shown in Fig. 3. The average composition of the dendritic structure and the matrix is also given in the Table 2. The dendrites are rich in Zr, Fe, Cr and the remaining area is rich in Zr, Fe, Ni. The dendritic phase is $ZrCr_2$–liquid (Zr,Fe) and Ni rich eutectic is Zr_2Fe–Zr_2Ni. The second region of molten zone, towards stainless steel, is mainly composed of a Zr_2Fe–Zr_2Ni phase and a few islands of dendritic structure $ZrCr_2$–liquid (Zr,Fe) and intermetallics $Zr(Cr,Fe)_2$ as shown in Fig. 4. Similar types of regions were formed, with a reduction in the size and area of the Laves phase $Zr(Cr,Fe)_2$, in samples welded for a shorter time. This reduction in area and size of the Laves phase is due to the shorter time available for the

diffusion of zirconium to stainless steel. The observed formation of the different regions can be explained on the basis of the mechanism proposed by Hofmann and Markiewicz [11] and Uetsuka et al. [12] for the diffusion bonding of Zircaloy-4 and a Ni-base alloy. The molten

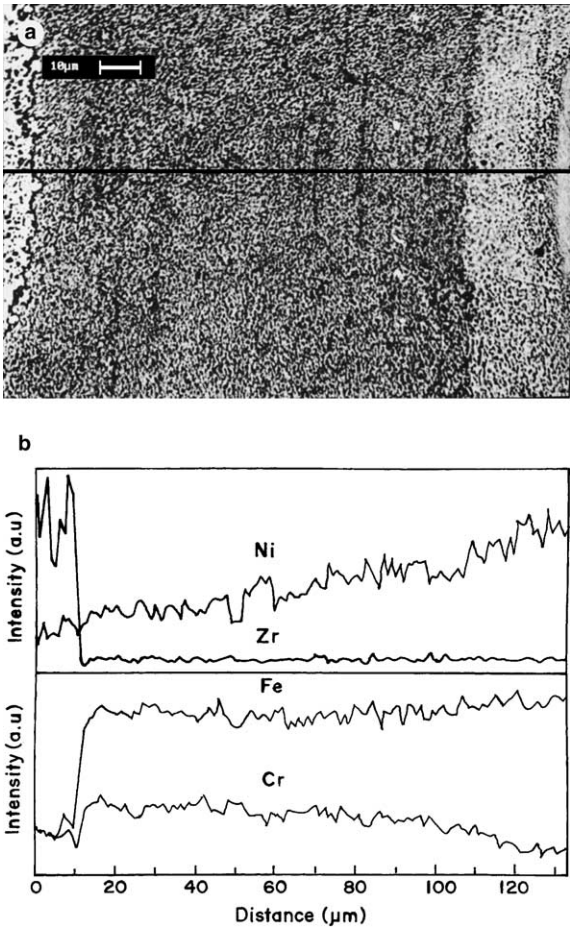

Fig. 2. (a) Back scattered electron micrograph of the HAZ on the side of stainless steel. (b) Line scan of Zr, Ni, Cr and Fe across the line in Fig. 2(a).

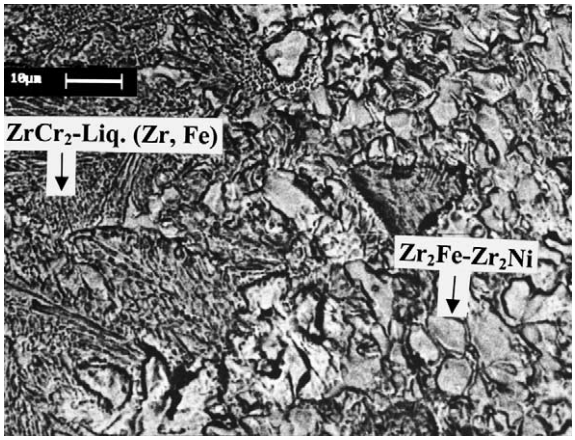

Fig. 3. SEM micrograph of dendritic structure on the side of Zircaloy-4.

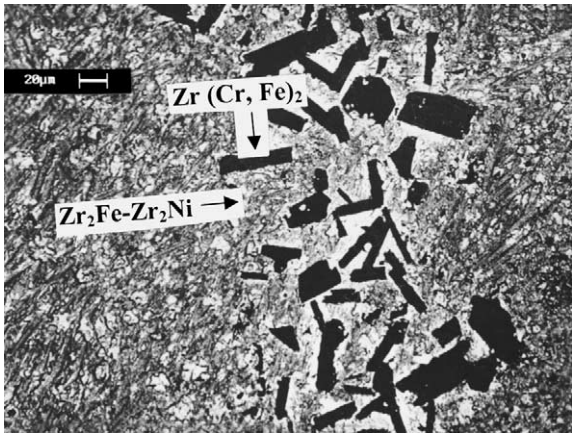

Fig. 4. SEM micrograph showing the Zr–Fe–Ni rich eutectic along with $Zr(Cr,Fe)_2$ intermetallics.

Table 2
Quantitative analysis of the phases and their hardness in Zircaloy-4 and stainless steel welded joints

Phases/eutectic	Elements	Concentration (wt%)	Phase	Hardness HV
Rod shape particles	Zr	50		
	Fe	29	$Zr(Cr,Fe)_2$	1300 ± 10
	Cr	21		
Molten zone with dendritic structure	Fe	14		
	Cr	8	$ZrCr_2$–liquid (Zr,Fe)	500 ± 10
	Zr	78		
Molten zone eutectic phase	Fe	17		
	Ni	5	Zr_2Fe–Zr_2Ni	400 ± 10
	Zr	78		

Table 3
Microhardness of HAZs and areas away from the molten zone

Alloys	Hardness HV in HAZs	Hardness HV outside the HAZ
Zircaloy-4	260 ± 10	200 ± 10
SS-304L	250 ± 10	145 ± 10

area near the HAZ in stainless steel consists of Zr-$(Cr,Fe)_2$, which is formed due to the diffusion of Zr from Zircaloy, while the matrix is Zr_2Fe–Zr_2Ni as Ni, Fe and Cr diffuse from stainless steel. As Ni diffuses faster than Cr towards the Zircaloy side, the HAZ on the side of stainless steel is found to be depleted in Ni but rich in Cr. The molten zone is found to have Zr_2Fe–Zr_2Ni and $ZrCr_2$–liquid (Zr,Fe) phases, which are formed because of the Zr–Cr, Zr–Ni, Zr–Fe eutectic reactions occurring during cooling. Eutectic reactions cause the formation of a liquid phase that penetrates along the boundaries of $Zr(Cr,Fe)_2$ and then decomposes, on cooling, into $ZrCr_2$–liquid (Zr,Fe) and Zr_2Fe–Zr_2Ni. The dendritic structure comprises of $ZrCr_2$–liquid (Zr,Fe) and the remaining portion is Zr_2Fe–Zr_2Ni. The measured compositions of these phases are close to those given in the tentative isothermal section of the Zr–Fe–Cr and Zr–Fe–Ni systems at 1000 °C [10]. The observed two regions within the molten zone are due to the difference in their cooling rates as the region near the Zircaloy side would cool earlier and hence it will have more dendrite formation than in the other region that takes longer time to cool. The results suggest that the brittle intermetallic compounds $Zr(Cr,Fe)_2$ are reduced in the weld zone and no cracks were observed as reported previously by TIG welding [8].

Values of microhardness of the HAZ close to the molten zone and on the area away from the molten zone are given in Table 3. The values in the HAZs are higher than those of the areas outside the heat effected zones. The increase in hardness in the heat affected zone in Zircaloy-4 near the molten zone may be due to the diffusion of a small amount of Fe, Cr and Ni. The increase in hardness in the HAZ in stainless steel near the molten zone is also due to diffusion of small amounts of Zr and Sn and reduction in Ni. The microhardness values of the areas in the molten zone containing different phases are given in Table 2. The hardness of the molten zone area near the stainless steel containing the $Zr(Cr,Fe)_2$ phase is three times higher than the average value of the molten zone. The hardness of the area containing the $ZrCr_2$–liquid (Zr,Fe) phase is also higher compared to areas of the Zr_2Fe–Zr_2Ni phase, which indicates that $ZrCr_2$–liquid (Zr,Fe) introduces more strain than the Zr_2Fe–Zr_2Ni phase.

4. Conclusions

Electron beam welding has produced phases like $Zr(Cr,Fe)_2$, $ZrCr_2$–liquid (Zr,Fe) and Zr_2Fe–Zr_2Ni in the molten zone. However, the formation of the harmful intermetallic compound $Zr(Cr,Fe)_2$ considered to be the major cause of cracking and produced in other welding techniques has been reduced considerably. The defects like porosity, voids and cracks were avoided. The heat-affected region on both sides of the molten zone is reduced in electron beam welding. The brittle nature of the $Zr(Cr,Fe)_2$ intermetallic compound is also confirmed from the hardness values that are three times higher than the major areas of the molten zone.

Acknowledgements

The authors are grateful to the members of the Radiation Damage Group, Nuclear Physics Division, for their assistance in the experimental work.

References

[1] J.B. Bai, C. Prioul, S. Lansiart, D. Francois, Scr. Metall. Mater. 25 (1991) 2559.
[2] M.H. Cooper, R. Serkes, M.G. Wright, INIS-MF-8473 (1981) 237.
[3] K. Bhanumurthy, J. Krishnan, G.B. Kale, S. Banerjee, J. Nucl. Mater. 217 (1994) 67.
[4] G. Perona, R. Sesini, W. Nicodemi, R. Zoja, J. Nucl. Mater. 18 (1966) 278.
[5] H.I. Shaaban, F.H. Hammad, J.L. Baron, J. Nucl. Mater. 71 (1978) 277.
[6] F.H. Hammad, H.I. Shaaban, J. Nucl. Mater. 80 (1979) 152.
[7] P.Gr. Lucuta, I. Patru, F. Vasiliu, J. Nucl. Mater. 99 (1981) 154.
[8] D. Mukherjee, J.P. Panakkal, J. Mater. Sci. Lett. 14 (1995) 1383.
[9] Zhou Hairong, Zhou Bangxin, CNIC-01108, SINRE-0067 (1996).
[10] H. Kleykamp, R. Pejsa, Kernforschungszentrum Karlsruhe, report KfK-4872 (1991).
[11] P. Hofmann, M. Markiewicz, Kernforschungszentrum Karlsruhe, report KfK-4729 (1994).
[12] H. Uetsuka, F. Nagase, T. Otomo, J. Nucl. Mater. 246 (1997) 180.